

Distinguishing black holes and wormholes with orbiting hot spots

Zilong Li and Cosimo Bambi*

Center for Field Theory and Particle Physics & Department of Physics, Fudan University, 200433 Shanghai, China

(Dated: December 3, 2024)

The supermassive black hole candidates at the center of every normal galaxy might be wormholes created in the early Universe and connecting either two different regions of our Universe or two different universes in a Multiverse model. Indeed, the origin of these supermassive objects is not well understood, topological non-trivial structures like wormholes are allowed both in general relativity and in alternative theories of gravity, and current observations cannot rule out such a possibility. In a few years, the VLTI instrument GRAVITY will have the capability to image blobs of plasma orbiting near the innermost stable circular orbit of SgrA*, the supermassive black hole candidate in the Milky Way. The secondary image of a hot spot orbiting around a wormhole is substantially different from the one of a hot spot around a black hole, because the photon capture sphere of the wormhole is much smaller, and its detection could thus test if the center of our Galaxy harbors a wormhole rather than a black hole.

PACS numbers: 04.20.-q, 04.70.-s, 98.35.Jk

I. INTRODUCTION

The Einstein equations are local equations relating the geometry of the spacetime to its matter content. There is no information about the spacetime topology. Even if it is far from our common sense, we cannot exclude that our Universe has a non-trivial topology or that it contains topologically non-trivial structures. In this spirit, there is a rich literature on wormholes (WHs); that is, short-cuts connecting two different regions of our Universe or two different universes in Multiverse theories [1]. WH spacetimes are allowed even in alternative theories of gravity. Since it is required a change of topology, WHs may not be created in the Universe today, but a number of mechanisms may have worked in the early Universe [2]. Primordial WHs may have survived till today and live somewhere in the Universe. In particular, they have been proposed as candidates for the supermassive objects that are seen at the center of every normal galaxy [3]. These objects are usually supposed to be Kerr black holes (BHs) with a mass $M \sim 10^5 - 10^9 M_\odot$, but their actual nature is not known.

In the case of the center of our Galaxy, the central supermassive object has a mass $M \approx 4 \cdot 10^6 M_\odot$ [4]. An upper bound on its radius can be inferred from the closest distance approached by the orbiting stars. Current data put this bound at about 45 AU, which corresponds to ~ 600 Schwarzschild radii [5]. Such an estimates of the mass and radius can exclude the possibility that the central object is actually a cluster of neutron stars, because the cluster lifetime would only be $\sim 10^5$ yrs, which is much shorter than the age of this system [5, 6]. The non-observations of thermal radiation emitted by the possible surface of this object may also be interpreted as an indication for the presence of an event/apparent horizon [7]. This body of evidence strongly supports the conclusion

that the supermassive object at the center of the Galaxy is a supermassive BH. Such a conclusion is naturally extended to all the supermassive objects in galactic nuclei. However, the origin of these BH candidates is not clear: we do not understand how they were able to become so heavy in a very short time, as we know BH candidates with a mass $M \sim 10^9 M_\odot$ at redshift $z \gtrsim 6$, i.e. just about 100 million years after the Big Bang [8]. Moreover, there is no real indication that the spacetime geometry around these objects is described by the Kerr solution [9] (for a review, see e.g. [10]).

While of exotic nature, at least some kinds of primordial WHs can be viable candidates to explain the supermassive objects at the center of galaxies. These objects have no solid surface, and therefore they may mimic the presence of an event horizon. They would have been produced in the early Universe and grown during inflation, so they could explain their presence even at very high redshift. It is therefore a natural question to wonder whether astrophysical observations can distinguish Kerr BHs and WHs and thus test the WH scenario. Despite the clear difference between BHs and WHs, current observations cannot rule out the possibility that the supermassive objects in galactic nuclei are WHs instead of BHs. In Ref. [11], one of us considered a particular family of traversable WHs and studied the possibility of distinguishing BHs and WHs from the analysis of the $K\alpha$ iron line. The latter is a very narrow emission line at about 6.4 keV, but the one observed in the spectra of supermassive BH candidates is broad and skewed, as a result of special and general relativistic effects. The analysis of this line is currently the only relatively robust technique to probe the spacetime geometry around these supermassive objects. In Ref. [11], it was found that the iron line profile produced in the accretion disk of a non-rotating WH looks like the one emitted from a disk around a Kerr BH with spin parameter $a_* \approx 0.8$. More in general, WHs with spin parameter $a_* \lesssim 0.02$ may be interpreted as Kerr BHs with spin parameter in the range

* Corresponding author: bambi@fudan.edu.cn

$a_* \approx 0.8 - 1.0$, while WHs with spin parameter larger than 0.02 have substantially different iron lines and can be ruled out because inconsistent with observations.

The possibility of observationally testing the idea that the supermassive objects in galactic nuclei are WHs was further discussed in Ref. [12], where it was pointed out that it would be relatively easy to figure out if SgrA* is a WH or a BH from the observation of its “shadow”. The latter is a dark area over a brighter background seen by a distant observer if the compact object is surrounded by optically thin emitting material and corresponds to the apparent photon capture sphere [13]. While the exact shape and size of the shadow of Kerr and non-Kerr BHs is extremely similar [14], and at present it is not completely clear if its future detection can constrain possible deviations from the Kerr solution, the shadow of a WH is much smaller than the one of a BH, and therefore distinguishable even without an accurate detection and with all the systematic effects that significantly tangle the job [12].

In the present paper, we further extend the study of Refs. [11, 12] and we investigate the possibility of testing if SgrA* is a WH by observing a hot blob of plasma orbiting near the innermost stable circular orbit (ISCO). Within a few years, NIR observations with GRAVITY will have the capability to directly image hot spots orbiting near the ISCO of SgrA* [15, 16], and open a new window to test the actual nature of this object. These data are supposed to come out before the first detection of the shadow. Because of the dramatically different size of the photon capture sphere of WHs and BHs, we find that the possible detection of the secondary image of a hot spot orbiting close to the compact object could test the possibility that SgrA* is a WH rather than a BH. Specific differences may also be present in the hot spot light curve and in the hot spot centroid track, but their features are more model-dependent: our hot spot model is too simple to conclude that their observation in real data can distinguish a WH from a BH, and further investigation based on more sophisticated and realistic models would be necessary.

II. HOT SPOT MODEL

SgrA* exhibits powerful flares in the X-ray, NIR, and sub-mm bands [17]. During a flare, the flux increases up to a factor 10. A flare typically lasts 1-3 hours and the rate is of a few events per day. These flares seem to show a quasi-periodic substructure on a time scale ranging from 13 to about 30 minutes. Several mechanisms have been proposed, such as the heating of electrons in a jet [18], Rossby wave instability in the disk [19], the adiabatic expansion of a blob of plasma [20], and blobs of plasma orbiting at the ISCO of SgrA* [21]. At least some authors have claimed that current observations favor the model of the hot spot near the ISCO [22]. Such a scenario is also supported by some general relativistic magneto-

hydrodynamic simulations of accretion flows onto BHs that show that temporary clumps of matter may be common in the region near the ISCO [23]. Within a few years, the GRAVITY instrument for the ESO Very Large Telescope Interferometer (VLTI) will have the capability to image blobs of plasma orbiting around SgrA* with an angular resolution of about $10 \mu\text{as}$ and a time resolution of about 1 minute [15, 16], and it will thus be possible to test the hot spot model.

For a Kerr BH with a mass $M = 4 \cdot 10^6 M_\odot$, the ISCO period ranges from about 30 minutes ($a_* = 0$) to 4 minutes ($a_* = 1$ and corotating orbit). The observed period of the quasi-periodic substructure of the flares of SgrA* ranges from 13 to about 30 minutes. If the hot spot model is correct, this means that the radius of the orbit of the hot spot may vary and be larger than the one of the ISCO. The shortest period ever measured is 13 ± 2 minutes. If we assume that the latter corresponds to the ISCO period, or at least that it is very close to it, one finds $a_* = 0.70 \pm 0.11$ for $M = 3.6 \cdot 10^6 M_\odot$ [22]. In Ref. [24], the authors claimed the presence of a quasi-periodic substructure with a period of 5 minutes, which was interpreted as an indication that SgrA* is rotating very fast, with a spin parameter close to 1. However, the analysis of the same data sets in [25] did not find such a short period substructure.

In the present work, we will consider the simplest hot spot model; that is, a single region of isotropic and monochromatic emission following a geodesic trajectory. Located on the equatorial plane, this hot spot is modeled as an optically thick emitting disk of finite radius. The local specific intensity of the radiation is chosen to have a Gaussian distribution in the local Cartesian space

$$I_{\text{em}}(\nu_{\text{em}}, x) \sim \delta(\nu_{\text{em}} - \nu_*) \exp \left[- \frac{|\tilde{\mathbf{x}} - \tilde{\mathbf{x}}_{\text{spot}}(t)|^2}{2R_{\text{spot}}^2} \right], \quad (1)$$

where ν_{em} is the photon frequency measured in the rest-frame of the emitter, while ν_* is the emission frequency of this monochromatic source. The spatial position 3-vector $\tilde{\mathbf{x}}$ is given in pseudo-Cartesian coordinates. Outside a distance of $4R_{\text{spot}}$ from the guiding geodesic trajectory $\tilde{\mathbf{x}}_{\text{spot}}$, there is no emission. Plausible values are $R_{\text{spot}} = 0.1 - 1.0M$, but it depends on the orbital radius and it is important to check that any point of the hot spot does not exceed the speed of light. The specific intensity of the radiation measured by the distant observer is given by

$$I_{\text{obs}}(\nu_{\text{obs}}, t_{\text{obs}}) = g^3 I_{\text{em}}(\nu_{\text{em}}, t_{\text{obs}}), \quad (2)$$

where g is the redshift factor

$$g = \frac{E_{\text{obs}}}{E_{\text{em}}} = \frac{\nu_{\text{obs}}}{\nu_{\text{em}}} = \frac{k_\alpha u_{\text{obs}}^\alpha}{k_\beta u_{\text{em}}^\beta}, \quad (3)$$

k^α is the 4-momentum of the photon, $u_{\text{obs}}^\alpha = (-1, 0, 0, 0)$ is the 4-velocity of the distant observer, and $u_{\text{em}}^\alpha = (u_{\text{em}}^t, 0, 0, \Omega u_{\text{em}}^t)$ is the 4-velocity of the emitter. Ω is the Keplerian angular frequency of a test-particle at the

emission radius r_e . $I_{\text{obs}}(\nu_{\text{obs}})/\nu_{\text{obs}}^3 = I_{\text{em}}(\nu_{\text{em}})/\nu_{\text{em}}^3$ follows from the Liouville theorem. The hot spot emission is assumed to be monochromatic and isotropic, with a Gaussian intensity, as shown in Eq. (1). Using the normalization condition $g_{\mu\nu}u_{\text{em}}^\mu u_{\text{em}}^\nu = -1$, one finds

$$u_{\text{em}}^t = -\frac{1}{\sqrt{-g_{tt} - 2g_{t\phi}\Omega - g_{\phi\phi}\Omega^2}}, \quad (4)$$

and therefore,

$$g = \frac{\sqrt{-g_{tt} - 2g_{t\phi}\Omega - g_{\phi\phi}\Omega^2}}{1 + \lambda\Omega}, \quad (5)$$

where $\lambda = k_\phi/k_t$ is a constant of the motion along the photon path. Doppler boosting and gravitational redshift are entirely encoded in the redshift factor g . The effect of light bending is included by the raytracing calculation.

The observer sky is divided into a number of small elements and the ray-tracing procedure provides the observed time-dependent flux density from each element. By integrating the observed specific intensity over the solid angle subtended by the image of the hot spot on the observer sky, we obtain the observed flux

$$\begin{aligned} F(\nu_{\text{obs}}, t_{\text{obs}}) &= \int I_{\text{obs}}(\nu_{\text{obs}}, t_{\text{obs}}) d\Omega_{\text{obs}} = \\ &= \int g^3 I_{\text{em}}(\nu_{\text{em}}, t_{\text{obs}}) d\Omega_{\text{obs}}. \end{aligned} \quad (6)$$

If we integrate over the frequency range of the radiation, we get the observed luminosity, or light curve, of the hot spot

$$L(t_{\text{obs}}) = \int F(\nu_{\text{obs}}, t_{\text{obs}}) d\nu_{\text{obs}}. \quad (7)$$

A more detailed description of the calculation procedure can be found, for instance, in Ref. [26]. In the present paper, we normalize the light curves by dividing the observed luminosity $L(t_{\text{obs}})$ by the corresponding maximum, since only the shape of the light curve can be used to determine the parameters of the model. Such a time-dependent emission signal can be added to a background intensity coming from the inner region of the steady state accretion disk. By definition, the hot spot will have a higher density and/or higher temperature and thus a higher emissivity than the background accretion disk, adding a small modulation to the total flux.

III. TESTING THE WORMHOLE SCENARIO

In the calculations of the electromagnetic radiation emitted by a hot spot, the spacetime metric determines the exact photon propagation from the hot spot to the distant observer, the redshift factor g in Eq. (5), and the value of the ISCO radius. There are many kinds of WHs proposed in the literature, but not all are viable supermassive BH candidates. For instance, some WHs have vanishing or negative effective gravitational mass. In the

present work, we adopt the same asymptotically-flat non-rotating traversable WH solution discussed in [11, 12], whose line element reads [27]

$$ds^2 = e^{2\Phi(r)} dt^2 - \frac{dr^2}{1 - \frac{b(r)}{r}} - r^2 d\theta^2 - r^2 \sin^2 \theta d\phi^2, \quad (8)$$

where $\Phi(r)$ and $b(r)$ are, respectively, the redshift and the shape functions. A common choice is $\Phi(r) = -r_0/r$, where r_0 is the WH throat radius and sets the scales of the system. r_0 is interpreted as the mass of the object in the Newtonian limit and in what follows will be indicated with M , just to use the same notation in the WH and BH cases. The shape function can be assumed of the form

$$b(r) = \frac{M^\gamma}{r^{\gamma-1}}, \quad (9)$$

where γ is a constant. In this paper, we consider the case $\gamma = 1$, but the observational signature that distinguishes WHs and BHs is independent of the value of γ .

Let us now compare the features of the electromagnetic radiation emitted by a blob of plasma orbiting around a WH and a BH. Since the hot spot orbital frequency is the simplest parameter to measure, we want to compare the following three cases:

1. A hot spot orbiting the traversable WH in Eq. (8) at some radius r_{WH} .
2. A hot spot orbiting at the ISCO radius of a Kerr BH with spin parameter such that its Keplerian orbital frequency Ω_{ISCO} is the same as the one of the hot spot orbiting the WH at the radius r_{WH} .
3. A hot spot orbiting a Kerr BH with spin parameter $a_* = 0.99$ at the equatorial circular orbit with radius r_{BH} , whose Keplerian orbital frequency Ω_{BH} is the same as the one of the other two cases.

Fig. 1 shows the light curves (total and primary image light curves, respectively with blue-solid and red-dashed lines) of hot spots orbiting a WH (top panels), a Kerr BH at the ISCO radius (central panels), and a Kerr BH with spin parameter $a_* = 0.99$ (bottom panels). In the top left panel, the hot spot around the WH is at the ISCO radius of the metric in Eq. (8), $r_{\text{WH}} = 2M$. In the top right panel, the hot spot is at the radius $r_{\text{WH}} = 3M$. It follows that in the central panels showing the light curves of a hot spot at the ISCO of a Kerr BH, the spin parameter of the latter is $a_* = 0.883911$ (left panel) and 0.673917 (right panel). In the bottom panels of the hot spot light curves around a Kerr BH with $a_* = 0.99$, the hot spot orbital radius is respectively $r_{\text{BH}} = 2.3807M$ (left panel) and $3.3973M$ (right panel). The most important difference between the WH and BH cases is that in the BH light curves there is a small bump marking the maximum intensity of the secondary image light curve, which is instead absent in the WH light curve. The effect is more pronounced when the hot spot is closer to the compact object and tends to disappear as the hot

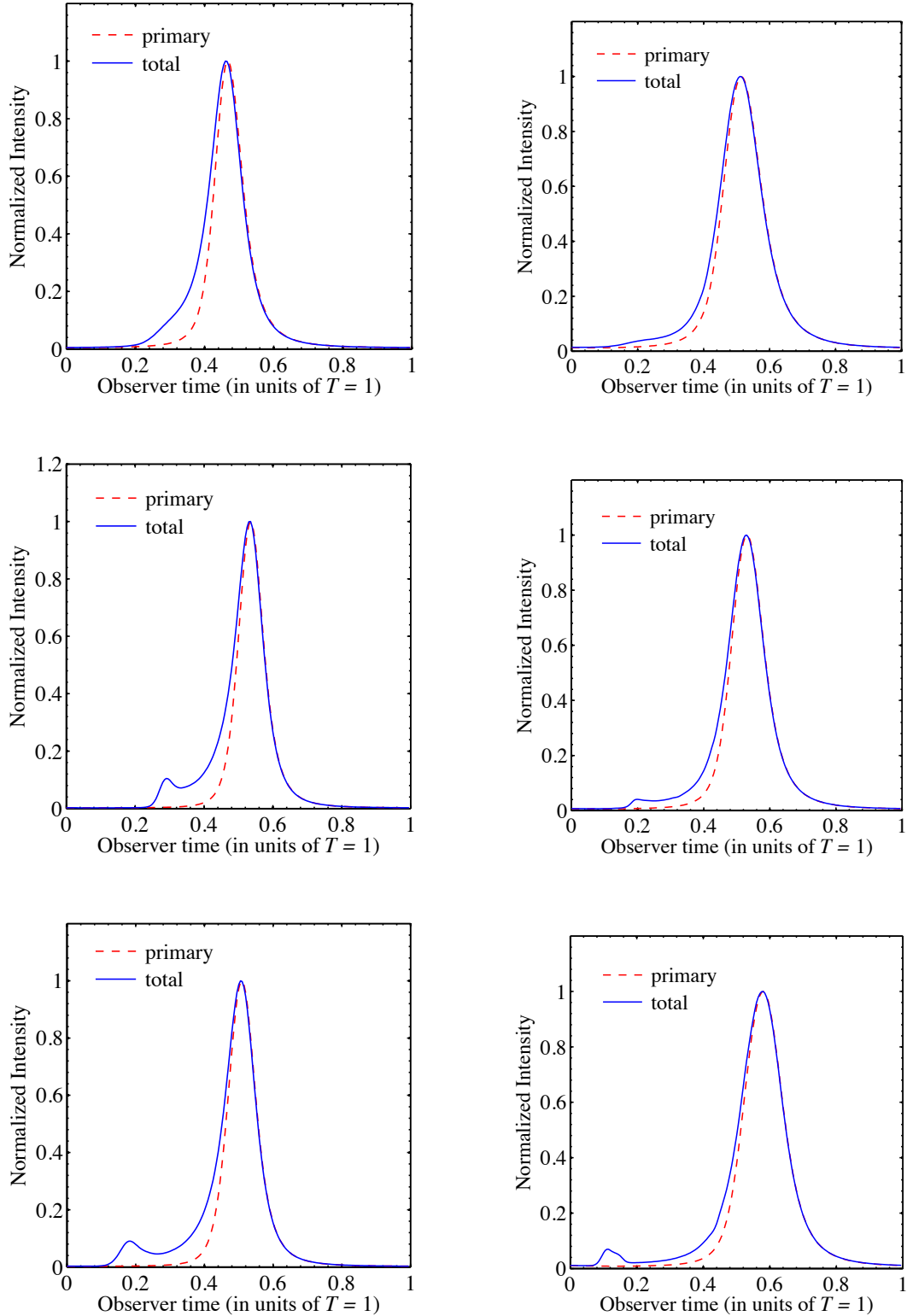


FIG. 1. Top panels: total light curves and primary image light curves of a hot spot orbiting around a WH at the ISCO $r_{\text{WH}} = 2M$ (left panel) and at the radius $r_{\text{WH}} = 3M$ (right panel). The viewing angle of the observer is $i = 60^\circ$ and the hot spot size is $R_{\text{spot}} = 0.15M$. Central panels: as in the top panels for a hot spot orbiting the ISCO of a Kerr BH with spin parameter $a_* = 0.883911$ (left panel) and $a_* = 0.673917$ (right panel); the value of the spin has been chosen to have an orbital frequency equal, respectively, to the one of a hot spot orbiting a WH at the ISCO and at the radius $r_{\text{WH}} = 3M$. Bottom panels: as in the top and central panels for a hot spot orbiting a Kerr BH with spin parameter $a_* = 0.99$ at the radius with the same Keplerian orbital frequency as the one of a hot spot orbiting a WH at the ISCO (left panel) and at the radius $r_{\text{WH}} = 3M$ (right panel). See the text for more details.

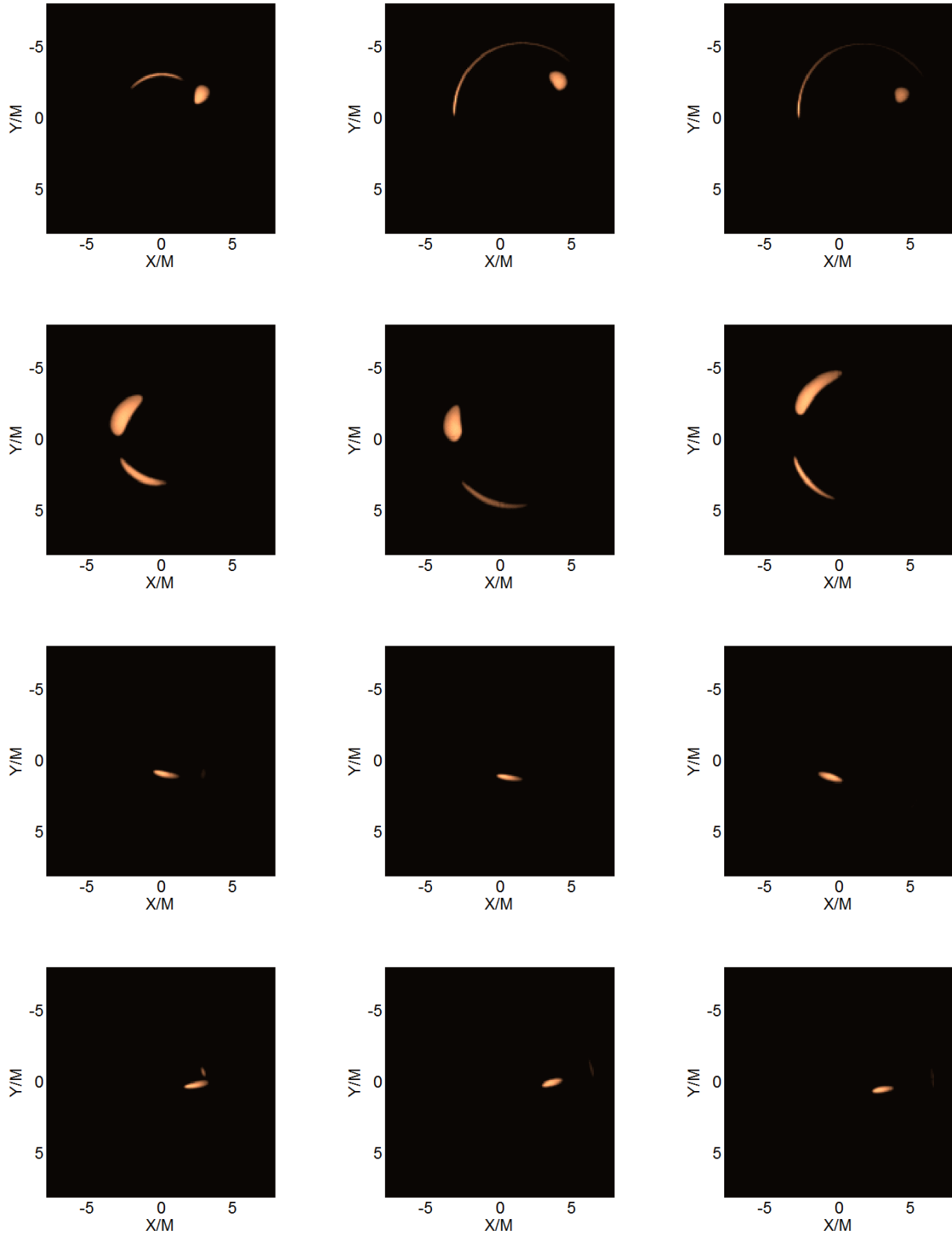


FIG. 2. Left panels: snapshots of a hot spot orbiting a WH at the ISCO. Central panels: snapshots of a hot spot orbiting a Kerr BH with spin parameter $a_* = 0.883911$ at the ISCO; the value of the spin parameter has been chosen to have the same orbital frequency as the one of the hot spot orbiting the ISCO of the WH. Right panel: snapshots of a hot spot orbiting a Kerr BH with spin parameter $a_* = 0.99$ at the radius with Keplerian orbital frequency equal to the frequency of the hot spots of the other two cases. The time interval between two adjacent panels in the same column is $T/4$, where T is the hot spot orbital period. In all these simulations, the inclination angle of the hot spot orbital plane with respect to the line of sight of the observer is $i = 60^\circ$ and the hot spot radius is $R_{\text{spot}} = 0.15 M$. See the text for more details.

spot radius/frequency increases. While such a feature in the hot spot light curve could potentially represent a clear observational signature to distinguish WHs and BHs, the actual properties of the bump due to the secondary image depend on the hot spot model (hot spot size, emissivity function, etc.). In Fig. 1, we have considered a single hot spot disk with radius $R_{\text{spot}} = 0.15 M$ and isotropic and monochromatic emission. The strong gravitational force near the compact object typically tends to destroy the hot spot, which is smeared along its orbit with the result to make the peaks of the images less well defined. Moreover, the substantial background may hide the small bump due to the secondary image in the BH light curves.

NIR observations may soon be able to directly image hot spots around SgrA*. For instance, the VLTI instrument GRAVITY is supposed to be operative within a few years and be able of astrometric measurements with an angular accuracy of about $10 \mu\text{arcsec}$ and a time resolution around 1 minute. Such a values have to be compared with the apparent gravitational radius of SgrA*, M , which is about $5 \mu\text{arcsec}$ for an object with a mass of 4 million Solar masses and a distance of 8 kpc from us, and with the hot spot orbital period, for which current data point out a time scale in the range 13 to 30 minutes (presumably due to the different orbital radius in different observations). Snapshots of the direct image of hot spots orbiting WHs and BHs are shown in Figs. 2 and 3. Every figure compares the three situations mentioned above, where the images of the hot spot around a WH are in the left column, the ones of a hot spot around a Kerr BH at the ISCO radius are in the central column, while the right column is for the images of a hot spot around a Kerr BH with spin parameter $a_* = 0.99$. Fig. 2 shows the cases in which the hot spot orbiting around the WH has orbital radius $r_{\text{WH}} = 2 M$, while Fig. 3 is for the WH hot spot with orbital radius $r_{\text{WH}} = 3 M$. We have thus the two scenarios already discussed in Fig. 1, and therefore the BH parameters are the same.

In all these snapshots, the secondary image is dimmer (in some snapshots almost absent) and smeared along/near the apparent photon capture radius. The apparent photon capture radius, i.e. the one seen by a distant observer, was computed in Ref. [12] in the case of the WH in Eq. (8) and it turns out to be about $2.718 M$. The angular size of the WH on the sky would be about $30 \mu\text{arcsec}$ for SgrA*. In the case of a Kerr BH, the apparent photon capture radius is about twice, with a small dependence on the BH spin and observer's inclination angle. For SgrA*, it would be around $50 \mu\text{arcsec}$. In particular the top panels in Figs. 2 and 3 clearly show the difference between the hot spot secondary images in the case of WHs and BHs. The primary images are pretty similar, while the secondary images are smeared along the apparent photon sphere, which is much smaller in the WH case. Let us also notice that such a prediction does not depend on the hot spot model (hot spot size, spectrum, observer's viewing angle, etc.), but only on the spacetime metric around the compact object. Its de-

tection can thus be considered as a clear observational signature to distinguish WHs and BHs. Let us also note that the apparent photon capture radius depends only on the redshift function $\Phi(r)$, while it is independent of the shape function $b(r)$ [12].

Lastly, we have computed the hot spot centroid tracks. Fig. 4 show 4 examples with different hot spot orbital period. The left panels show the two cases discussed in Figs. 1-3, in which the hot spot around the WH has orbital radius $r_{\text{WH}} = 2 M$ (top left panel in Fig. 4) and $r_{\text{WH}} = 3 M$ (bottom left panel in Fig. 4). In the top right panel in Fig. 4, the hot spot around the WH has orbital radius $r_{\text{WH}} = 2.5 M$, while in the bottom right panel the orbital radius is $r_{\text{WH}} = 4 M$. In Fig. 4, the hot spot size is $R_{\text{spot}} = 0.15 M$ and the observer's viewing angle is still $i = 60^\circ$. While one may be tempted to argue that the centroid track of WHs and BHs present different features, and therefore that its detection can distinguish WHs and BHs, as discussed in Ref. [21] the exact hot spot model is quite important. Since we are considering here a very simple model, it is not possible to figure out if the detection of the centroid track can be used to distinguish WHs and BHs.

IV. SUMMARY AND CONCLUSIONS

WHs are topologically non-trivial structures connecting either two different regions of our Universe or two different universes in a Multiverse model. While of exotic nature, they are allowed in general relativity and in alternative theories of gravity and they are viable candidates to explain the supermassive objects harbored at the center of every normal galaxy. In the present paper, we have extended the studies of Refs. [11, 12] and we have further investigated if observations can test the possibility that the supermassive BH candidates in galactic nuclei are instead WHs. We have focused our attention on the specific case of the metric in Eq. (8), which describes an asymptotically-flat non-rotating traversable WH. In Ref. [11], it was found that such a WH would be consistent with current observations of the $K\alpha$ iron line detected in the X-ray spectrum of supermassive BH candidates. In Ref. [12], it was pointed out that the observation of the shadow of SgrA*, the supermassive BH candidate at the center of the Milky Way, could easily test the possibility that this object is actually a WH rather than a BH, because the size of the shadow, which corresponds to the apparent photon capture sphere, is much smaller in the WH case than in the BH one.

In this paper, we have discussed the possibility of testing the presence of a WH at the center of our Galaxy by observing a hot blob of plasma orbiting near the ISCO of SgrA*. Such a kind of observations are expected to be soon possible in the NIR, before the first detection of the shadow of SgrA*, thanks to the advent of the VLTI instrument GRAVITY. We have found that the features of the hot spot secondary image are substantially different

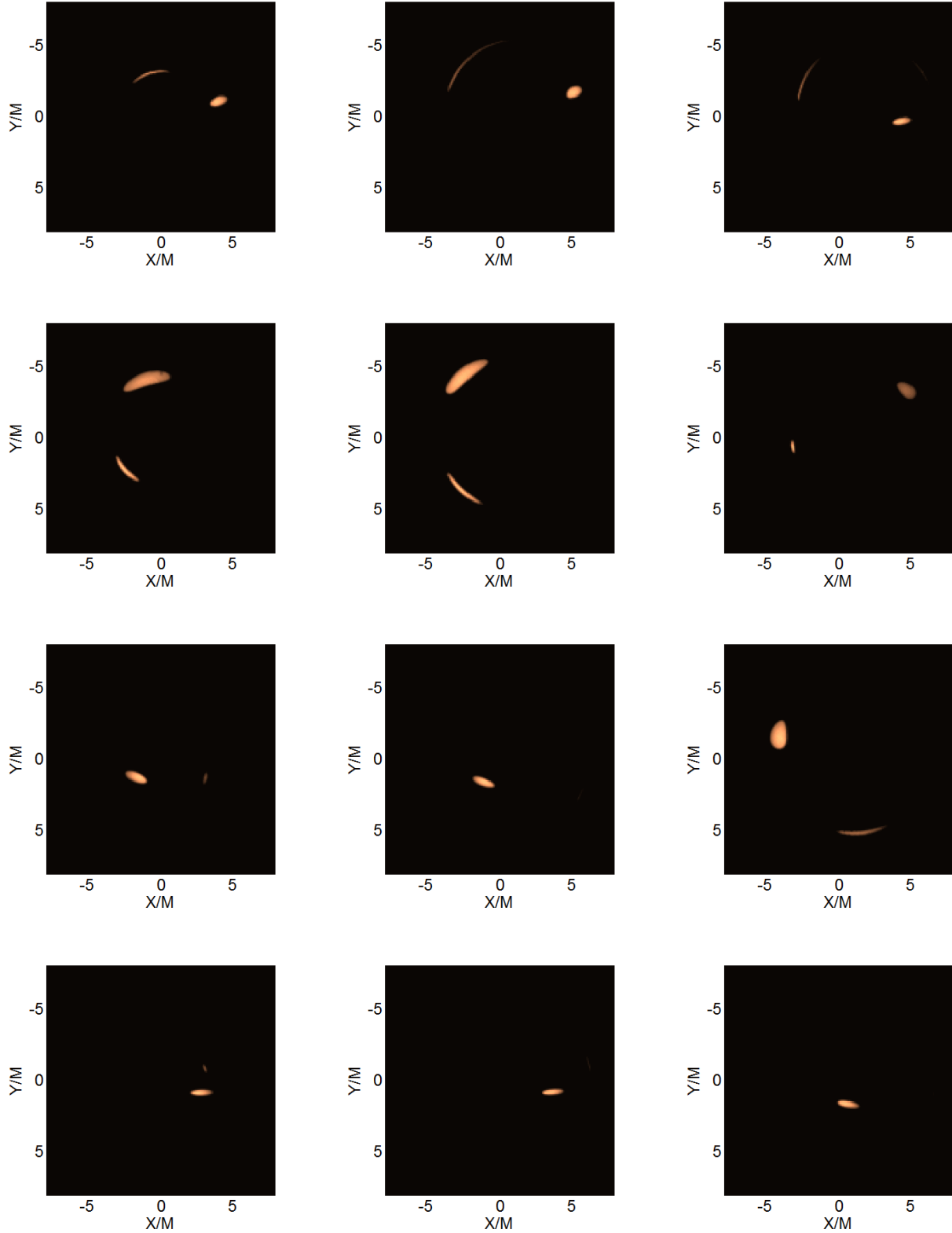


FIG. 3. As in Fig. 2 for a hot spot orbiting a WH at the radius $r_{\text{WH}} = 3M$ (left panels), a Kerr BH with spin parameter $a_* = 0.673917$ at the ISCO (central panels; the value of the spin parameter has been chosen to have the same hot spot orbital period as the one around the WH), and a Kerr BH with spin parameter $a_* = 0.99$ and at the radius with Keplerian orbital period equal to the one of the other two cases (right panels). See the text for more details.

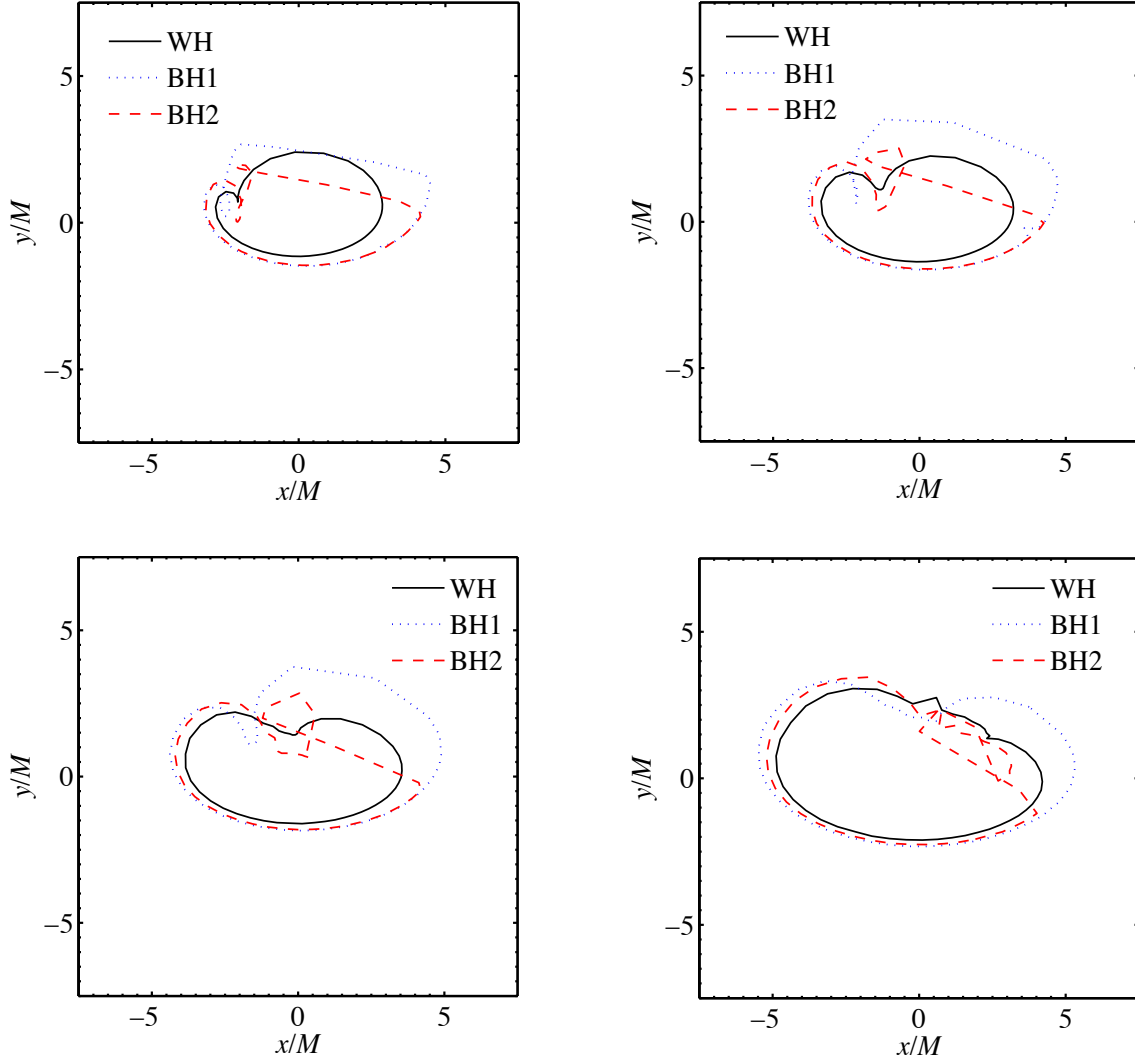


FIG. 4. Centroid tracks of a hot spot orbiting a WH (black-solid curves), a BH at the ISCO radius with spin parameter such that the hot spot orbital frequency is the same as the one around the WH (blue-dotted curves), and a BH with spin parameter $a_* = 0.99$ and at the radius with the same Keplerian orbital frequency as the one of the hot spots in the other two cases (red-dashed curves). The orbital radius of the hot spot around the WH is $r_{\text{WH}} = 2M$ (ISCO radius; top left panel), $r_{\text{WH}} = 2.5M$ (top right panel), $r_{\text{WH}} = 3M$ (bottom left panel), and $r_{\text{WH}} = 4M$ (bottom right panel). The inclination angle of the hot spot orbital plane with respect to the observer is $i = 60^\circ$ and the hot spot size is $R_{\text{spot}} = 0.15M$. See the text for more details.

between a WH and a BH and they probably represent the key-point to distinguish the two scenarios. If the hot spot is close to the compact object, even if not necessarily at the ISCO radius, the secondary image shows up around the apparent photon capture sphere, which is significantly different in the two spacetimes. The size of the WH photon capture radius projected on the observer sky is indeed about half the BH one and in the case of SgrA* they correspond, respectively, to about 30 and 50 μ arcsec. The detection of the direct image of the secondary image of a hot spot could thus test if SgrA* is a WH rather than a BH. Such a prediction is very general, in the sense that it does not depend on the hot spot model and on the inclination angle of the hot spot orbital plane with respect to the line of sight of the observer. The apparent photon capture radius only depends

on the spacetime geometry close to the compact object. Specific features of the secondary image are also encoded in the hot spot light curve and in its centroid track. However, these features do depend on the hot spot model and within our simple set-up it is not possible to figure out if future observations of light curves and centroid tracks can distinguish WHs and BHs.

ACKNOWLEDGMENTS

This work was supported by the NSFC grant No. 11305038, the Shanghai Municipal Education Commission grant for Innovative Programs No. 14ZZ001, the Thousand Young Talents Program, and Fudan University.

-
- [1] M. Visser, Phys. Rev. D **39**, 3182 (1989) [arXiv:0809.0907 [gr-qc]]; M. Visser, Phys. Rev. D **41**, 1116 (1990).
- [2] H. Kodama, M. Sasaki, K. Sato and K. -i. Maeda, Prog. Theor. Phys. **66**, 2052 (1981); D. Garfinkle and A. Strominger, Phys. Lett. B **256**, 146 (1991).
- [3] J. Kormendy and D. Richstone, Ann. Rev. Astron. Astrophys. **33**, 581 (1995).
- [4] S. Gillessen, F. Eisenhauer, S. Trippe, T. Alexander, R. Genzel, F. Martins and T. Ott, Astrophys. J. **692**, 1075 (2009) [arXiv:0810.4674 [astro-ph]].
- [5] A. M. Ghez, S. Salim, S. D. Hornstein, A. Tanner, M. Morris, E. E. Becklin and G. Duchene, Astrophys. J. **620**, 744 (2005) [astro-ph/0306130].
- [6] E. Maoz, Astrophys. J. **494**, L181 (1998) [astro-ph/9710309].
- [7] A. E. Broderick, A. Loeb and R. Narayan, Astrophys. J. **701**, 1357 (2009) [arXiv:0903.1105 [astro-ph.HE]].
- [8] X. Fan *et al.* [SDSS Collaboration], Astron. J. **122**, 2833 (2001) [astro-ph/0108063]; D. J. Mortlock *et al.*, Nature **474**, 616 (2011) [arXiv:1106.6088 [astro-ph.CO]].
- [9] C. Bambi, Phys. Rev. D **83**, 103003 (2011) [arXiv:1102.0616 [gr-qc]]; C. Bambi, Phys. Rev. D **85**, 043001 (2012) [arXiv:1112.4663 [gr-qc]]; C. Bambi, Phys. Lett. B **705**, 5 (2011) [arXiv:1110.0687 [gr-qc]]; C. Bambi, Phys. Rev. D **87**, 023007 (2013) [arXiv:1211.2513 [gr-qc]].
- [10] C. Bambi, Mod. Phys. Lett. A **26**, 2453 (2011) [arXiv:1109.4256 [gr-qc]]; C. Bambi, Astron. Rev. **8**, 4 (2013) [arXiv:1301.0361 [gr-qc]].
- [11] C. Bambi, Phys. Rev. D **87**, no. 8, 084039 (2013) [arXiv:1303.0624 [gr-qc]].
- [12] C. Bambi, Phys. Rev. D **87**, 107501 (2013) [arXiv:1304.5691 [gr-qc]].
- [13] H. Falcke, F. Melia and E. Agol, Astrophys. J. **528**, L13 (2000) [astro-ph/9912263].
- [14] C. Bambi and N. Yoshida, Class. Quant. Grav. **27**, 205006 (2010) [arXiv:1004.3149 [gr-qc]]; C. Bambi, F. Caravelli and L. Modesto, Phys. Lett. B **711**, 10 (2012) [arXiv:1110.2768 [gr-qc]]; Z. Li and C. Bambi, JCAP **1401**, 041 (2014) [arXiv:1309.1606 [gr-qc]]; N. Tsukamoto, Z. Li and C. Bambi, arXiv:1403.0371 [gr-qc].
- [15] F. Eisenhauer *et al.*, The Messenger **143**, 16 (2011); F. H. Vincent *et al.*, Mon. Not. Roy. Astron. Soc. **412**, 2653 (2011) [arXiv:1011.5439 [astro-ph.GA]].
- [16] <http://www.mpe.mpg.de/ir/gravity>
- [17] R. Genzel *et al.*, Nature **425**, 934 (2003) [astro-ph/0310821]; A. M. Ghez *et al.*, Astrophys. J. **601**, L159 (2004) [astro-ph/0309076]; A. Eckart *et al.*, Astron. Astrophys. **427**, 1 (2004) [astro-ph/0403577]; K. Dodds-Eden *et al.*, Astrophys. J. **728**, 37 (2011) [arXiv:1008.1984 [astro-ph.GA]]; G. Trap *et al.*, Astron. Astrophys. **528**, A140 (2011) [arXiv:1102.0192 [astro-ph.HE]].
- [18] S. Markoff, H. Falcke, F. Yuan and P. L. Biermann, Astron. Astrophys. **379**, L13 (2001) [astro-ph/0109081].
- [19] M. Tagger and F. Melia, Astrophys. J. **636**, L33 (2006) [astro-ph/0511520].
- [20] F. Yusef-Zadeh, D. Roberts, M. Wardle, C. O. Heinke and G. C. Bower, Astrophys. J. **650**, 189 (2006) [astro-ph/0603685].
- [21] N. Hamaus *et al.*, Astrophys. J. **692**, 902 (2009) [arXiv:0810.4947 [astro-ph]].
- [22] S. Trippe *et al.*, Mon. Not. Roy. Astron. Soc. **375**, 764 (2007) [astro-ph/0611737].
- [23] J. -P. De Villiers, J. F. Hawley and J. H. Krolik, Astrophys. J. **599**, 1238 (2003) [astro-ph/0307260]; J. D. Schnittman, J. H. Krolik and J. F. Hawley, Astrophys. J. **651**, 1031 (2006) [astro-ph/0606615].
- [24] B. Aschenbach, N. Grosso, D. Porquet and P. Predehl, Astron. Astrophys. **417**, 71 (2004) [astro-ph/0401589].
- [25] G. Belanger, R. Terrier, O. C. De Jager, A. Goldwurm and F. Melia, J. Phys. Conf. Ser. **54**, 420 (2006) [astro-ph/0604337].
- [26] Z. Li, L. Kong and C. Bambi, arXiv:1401.1282 [gr-qc].
- [27] T. Harko, Z. Kovacs and F. S. N. Lobo, Phys. Rev. D **78**, 084005 (2008) [arXiv:0808.3306 [gr-qc]].